Absorbed dose to water reference dosimetry using solid phantoms in the context of absorbed-dose protocols

Jan Seuntjens,[a] Marina Olivares, Michael Evans, and Ervin Podgorsak
Department of Medical Physics, McGill University Health Centre, 1650 Cedar av., Montreal, H3G 1A4, Canada

(Received 1 February 2005; revised 9 July 2005; accepted for publication 11 July 2005; published 26 August 2005)

For reasons of phantom material reproducibility, the absorbed dose protocols of the American Association of Physicists in Medicine (AAPM) (TG-51) and the International Atomic Energy Agency (IAEA) (TRS-398) have made the use of liquid water as a phantom material for reference dosimetry mandatory. In this work we provide a formal framework for the measurement of absorbed dose to water using ionization chambers calibrated in terms of absorbed dose to water but irradiated in solid phantoms. Such a framework is useful when there is a desire to put dose measurements using solid phantoms on an absolute basis. Putting solid phantom measurements on an absolute basis has distinct advantages in verification measurements and quality assurance. We introduce a phantom dose conversion factor that converts a measurement made in a solid phantom and analyzed using an absorbed dose calibration protocol into absorbed dose to water under reference conditions. We provide techniques to measure and calculate the dose transfer from solid phantom to water. For an Exradin A12 ionization chamber, we measured and calculated the phantom dose conversion factor for six Solid Water™ phantoms and for a single Lucite phantom for photon energies between ^{60}Co and 18 MV photons. For Solid Water™ of certified grade, the difference between measured and calculated factors varied between 0.0% and 0.7% with the average dose conversion factor being low by 0.4% compared with the calculation whereas for Lucite, the agreement was within 0.2% for the one phantom examined. The composition of commercial plastic phantoms and their homogeneity may not always be reproducible and consistent with assumed composition. By comparing measured and calculated phantom conversion factors, our work provides methods to verify the consistency of a given plastic for the purpose of clinical reference dosimetry. [DOI: 10.1118/1.2012807]

Key words: absorbed dose reference dosimetry, plastic phantoms, dose conversion, scaling, Monte Carlo dose calculations

I. INTRODUCTION

Most recent national and international megavoltage dosimetry protocols [e.g., AAPM TG-51 (Ref. 1) and IAEA TRS-398 (Ref. 2)] are based on reference dose measurements in water phantoms. The recommended detector is an air-filled ionization chamber for which an absorbed dose-to-water calibration coefficient traceable to a standards laboratory has been established. For the AAPM TG-51 protocol this calibration coefficient is obtained in a cobalt-60 beam. A number of papers have dealt with the rational and with beam quality specification issues associated with these water-based protocols (see, for example, Refs. 3–6). Water has been chosen as reference phantom material since it is well-defined and reproducibly available.

There are situations for which dose measurements in water are impractical. An example of this is the dosimetric quality assurance of the output of therapy machines which must be verified routinely and for these occasions solid phantoms are set up more quickly and reproducibly. Following a megavoltage photon or electron beam calibration using an appropriate absorbed dose protocol (e.g., TG-51), the combined "ionization chamber-solid phantom monitoring device" is calibrated and subsequently used for performing the routine beam output measurements. This process is essentially a verification of beam constancy and bears no direct physical connection with the reference absorbed dose-to-water measurement. In principle, one can use any phantom material and any chamber type for this purpose provided the stability of the components is ensured and maintained. However, in general, different chambers and phantoms are not interchangeable and therefore, upon a chamber failure, one needs to reestablish the absorbed dose-to-water calibration using a water phantom and a calibrated chamber to assess the response of the new "chamber-phantom" device. The interchangeability of chambers and phantoms is even less ensured if the routine output measurement setup departs more drastically from the reference in water setup. Having a solid phantom-based setup in which there is a direct and physically clear link with the reference dosimetry setup adds possibilities for clinical verification and quality assurance.

With the outdated N_{gas} or $N_{D,\mathrm{air}}$ concepts that were explicitly part of the air-kerma based protocols such as the AAPM TG-21 protocol[7] or IAEA TRS-277 protocol,[8] the chamber used in the calibration protocol was characterized with respect to its own sensitive volume. So, once a N_{gas} or $N_{D,\mathrm{air}}$ had been determined, any chamber could be used to replace

the defective chamber as long as the data to reestablish absorbed dose to water from a measurement in a water or plastic phantom were explicitly provided and there was no procedural difference between the quality assurance protocol and the reference dosimetry protocol. With the absorbed dose calibration protocols, these data and procedures are no longer explicitly part of the reference dosimetry protocol; yet, the degrees of freedom one has for making choices about solid phantoms do not prevent the user from making a reasonable choice of phantom material, depth in phantom, and other irradiation parameters so as to create conditions under which a measurement in a solid phantom can be directly converted into absorbed dose to water, if the need arises.

In this paper we discuss methods to determine absorbed dose to water from ionization chamber measurements in a solid phantom within the context of absorbed dose calibration protocols. We provide a method to uncouple chamber specific properties from characteristics of water-equivalent solid phantom materials and a simple technique to experimentally measure the factor involved in transferring dose from solid phantoms to water. The methods used in this paper use similar principles as the work revolving around dose conversion from graphite to water that formed the basis of the United Kingdom standards for absorbed dose to water in photon and electron beams.[9] Dose conversion and the use of solid phantoms in reference dosimetry has also been discussed to some extent in certain absorbed dose-based dosimetry protocols[10,11] although, for photon beams, no practical clinical recipe has been given.

II. BACKGROUND

In the following we present the formal framework for absorbed dose-to-water determination using ionization chamber measurements in solid phantoms in the context of absorbed-dose-to-water protocols.

A. Dose transfer calibration coefficient

We define the *dose transfer calibration coefficient* $(N_{D,w}^{Q})_s$ as

$$(N_{D,w}^{Q})_s = \frac{D_w^Q}{M_s^Q}, \tag{1}$$

where D_w^Q is the dose to water at the reference depth z_{ref} in the water phantom and M_s^Q is the chamber reading at a suitable equivalent depth z_{eq} in the Solid Water™ phantom, corrected for the standard influence quantities (ambient air temperature, pressure and humidity; applied chamber voltage and polarity; chamber leakage currents and stem effects). Both D_w^Q and M_s^Q are obtained for the same monitor unit (MU) setting, same nominal field size of 10×10 cm^2, and same nominal source-surface distances (SSD) of 100 cm.

The dose transfer calibration coefficient $(N_{D,w}^{Q})_s$ applicable to a given chamber/solid phantom combination, allows the conversion of a chamber reading in a solid phantom to absorbed dose to water D_w^Q at the reference depth z_{ref} in water by multiplying the chamber solid phantom reading M_s^Q (corrected for influence quantities and obtained at depth z_{eq} in solid phantom) with the dose transfer coefficient $(N_{D,w}^{Q})_s$. In $(N_{D,w}^{Q})_s$, Q stands for the beam type (megavoltage x rays or megavoltage electrons) and quality; the subscript D,w for dose to water; and subscript s for solid phantom.

B. Phantom dose conversion factor

The absorbed-dose in solid phantom D_s^Q is related to the reading of the ionization chamber in that phantom by

$$D_s^Q = M_s^Q N_{\mathrm{gas}} \left(\frac{\bar{L}}{\rho}\right)_{\mathrm{air}}^{s} (P_Q)_s, \tag{2}$$

where M_s^Q is the chamber reading corrected for influence quantities, N_{gas} is the cavity gas calibration coefficient, $(\bar{L}/\rho)_{\mathrm{air}}^{s}$ the average restricted collision stopping power ratio, solid phantom to air, and $(P_Q)_s$ the overall perturbation correction factor of the ionization chamber in the solid phantom at the megavoltage beam quality Q.

For a chamber calibrated in terms of absorbed dose to water, the relationship between $N_{D,w}^{Q}$, the absorbed dose calibration coefficient at beam quality Q, and N_{gas} is as follows:

$$N_{D,w}^{Q} = N_{D,w}^{\mathrm{Co}} k_Q = N_{\mathrm{gas}} \left(\frac{\bar{L}}{\rho}\right)_{\mathrm{air}}^{w} (P_Q)_w, \tag{3}$$

where $N_{D,w}^{\mathrm{Co}}$ is the absorbed dose to water calibration coefficient in a cobalt-60 beam; k_Q is the beam quality conversion factor; N_{gas} the cavity gas calibration coefficient; $(\bar{L}/\rho)_{\mathrm{air}}^{w}$ the average restricted collision mass stopping power ratio water-to-air; and $(P_Q)_w$ the overall perturbation correction factor for the ionization chamber in water.

By solving Eq. (3) for N_{gas} and inserting the resulting N_{gas} expression into Eq. (2), the dose-to-solid phantom can be expressed as

$$D_s^Q(z_{\mathrm{eq}}) = M_s^Q N_{D,w}^{\mathrm{Co}} k_Q \frac{\left(\frac{\bar{L}}{\rho}\right)_{\mathrm{air}}^{s} P_{Q,s}}{\left(\frac{\bar{L}}{\rho}\right)_{\mathrm{air}}^{w} P_{Q,w}}. \tag{4}$$

Equation (4) is valid at any depth as long as the conversion and correction factors can be evaluated. The depth of interest in the solid phantom is z_{eq}, an equivalent depth to the reference depth in water (see below). Thus, D_w^Q, the absorbed dose to water at depth z_{ref} can be determined from a measurement of D_s^Q in a solid phantom at depth z_{eq} using the following expansion of Eq. (4):

$$D_w^Q(z_{\mathrm{ref}}) = M_s^Q N_{D,w}^{\mathrm{Co}} k_Q \times \left[\left(\frac{D_w^Q(z_{\mathrm{ref}})}{D_s^Q(z_{\mathrm{eq}})}\right) \left(\frac{\left(\frac{\bar{L}}{\rho}(z_{\mathrm{eq}})\right)_{\mathrm{air}}^{s} P_{Q,s}(z_{\mathrm{eq}})}{\left(\frac{\bar{L}}{\rho}(z_{\mathrm{ref}})\right)_{\mathrm{air}}^{w} P_{Q,w}(z_{\mathrm{ref}})} \right) \right], \tag{5}$$

where the ratio of doses, (D_w^Q/D_s^Q), for the same primary beam impinging on both phantoms can be calculated either

by Monte Carlo methods or by using a scaling method (see, e.g., Ref. 12).

The term in square brackets in Eq. (5) can be defined as a *solid phantom-to-water dose conversion factor or, abbreviated, the phantom dose conversion factor* $k^Q_{s,w}$; i.e.,

$$k^Q_{s,w} = \left(\frac{D^Q_w(z_{\mathrm{ref}})}{D^Q_s(z_{\mathrm{eq}})}\right)\left(\frac{\left(\frac{\bar{L}}{\rho}(z_{\mathrm{eq}})\right)^s_{\mathrm{air}} P_{Q,s}(z_{\mathrm{eq}})}{\left(\frac{\bar{L}}{\rho}(z_{\mathrm{ref}})\right)^w_{\mathrm{air}} P_{Q,w}(z_{\mathrm{ref}})}\right), \tag{6}$$

so that, using Eqs. (1), (5), and (6), the calibration coefficient $(N^Q_{D,w})_s$ can be calculated from an absorbed dose-to-water calibration coefficient for cobalt-60 using the following simple expression:

$$(N^Q_{D,w})_s = N^{\mathrm{Co}}_{D,w} k_Q k^Q_{s,w}. \tag{7}$$

Despite the involvement of chamber perturbation correction factors, the solid phantom-to-water conversion factor $k^Q_{s,w}$ is only weakly dependent on the chamber type used, provided the chamber and phantom materials are not too dissimilar. However, the solid phantom-to-water conversion factor depends strongly on other conditions i.e., depth, field size) under which the chamber is irradiated in the solid phantom and therefore it is desirable to choose solid phantom irradiation conditions such that the factor can be determined accurately.

The relations presented so far apply to both megavoltage photon and electron beams. However, the appropriate choice for the depth of measurement will be different for each method. For megavoltage photon beams z_{eq} is the depth "equivalent" to the reference depth z_{ref} in the water phantom. In megavoltage electron beams recommendations for the equivalent reference depth z_{eq} have been given in the TRS-398 protocol. However, for practical reasons, the depth of measurement in the solid phantom is often at $z_{\max}$, the depth of maximum dose in the solid phantom for the particular electron beam and the dose transfer factor has to take into account the effect of the difference in depth between $z_{\max}$ and the true equivalent depth.

In the remainder of this paper we will present the determination of the equivalent depth and the calculation of the dose transfer factor for megavoltage photon beams only. Our work for electron beams is left for a future contribution.

C. Calculation of equivalent depth and $k^Q_{s,w}$ for megavoltage photon beams

To calculate the dose ratio in Eq. (6) for photon beams, use can be made of the scaling theorem[12] which forms the basis of absorbed dose-to-water standards disseminated by some primary standards laboratories.[13] The theorem states that: *(i) If two blocks of different materials are irradiated by the same photon beam and (ii) if irradiation geometry (field size, phantom dimensions) are scaled in the inverse ratio of electron densities of the two media, then, assuming that all photon interactions take place by Compton scatter, at corresponding scaled points of measurement in the two media the photon fluences are related through the inverse square law*. When all dimensions (SSD, field size, and depth) of the irradiation geometry have been scaled in the inverse ratio of electron density, the application of this theorem[12] relates the photon energy fluence ψ_w at depth z_{ref} in water-to-photon energy fluence ψ_s at depth z_{eq} in the solid phantom through an inverse square relationship as follows:

$$\frac{\psi_w(z_{\mathrm{ref}}, r_{\mathrm{ref}})}{\psi_s(z_{\mathrm{eq}}, r_{\mathrm{eq}})} = \left(\frac{f_{\mathrm{eq}} + z_{\mathrm{eq}}}{f_{\mathrm{ref}} + z_{\mathrm{ref}}}\right)^2, \tag{8}$$

where f_{eq} and f_{ref} represent the equivalent and the reference source-surface distances (SSD) for the two phantoms, respectively. The equality expressed in Eq. (8) is not exact, because of the small effect of air attenuation as well as the contribution of pair production to photon attenuation in phantoms. However, these effects are minor and can be ignored in the first approximation. In the application of the fluence scaling theorem it is assumed that upon scaling the field dimensions (SSD and, as a result of that, field size), the incoming primary energy fluence on the central axis is not altered. Nutbrown *et al.*[14] have shown that it is possible to scale depth and SSD for constant collimator settings to arrive at accurate dose conversions water to graphite in clinical beams. In addition to changing measurement depth this approach requires changing SSD by an amount dictated by the electron density of an individual phantom relative to water, which is somewhat impractical in the clinical setting. When changing the field size at constant SSD by changing collimator (jaw) opening, however, the primary photon energy fluence will be modified due to collimator scattering and would render the scaling method invalid. To simplify the setup of a solid phantom in the context of verification measurements and to avoid the introduction of collimator factors we have opted to keep the field size and SSD for irradiation of the solid phantoms the same as in the reference conditions (i.e., 10×10 cm^2 and 100 cm, respectively). By doing so, we are slightly underestimating or overestimating phantom scattering in a solid with lower or higher electron density than water, respectively. To account for this scatter deficiency (or scatter excess) at constant SSD we need to correct the energy fluence by introducing phantom scatter factors. For application of the fluence scaling theorem at constant SSD (and field size), the fluence in the solid phantom thus needs to be corrected to account for the difference in phantom scattering as a result of leaving this portion of the irradiation geometry unmodified. Hence Eq. (8) becomes

$$\frac{\psi_w(z_{\mathrm{ref}}, r_{\mathrm{ref}})}{\psi_s(z_{\mathrm{eq}}, r_{\mathrm{ref}})} = \left(\frac{f + z_{\mathrm{eq}}}{f + z_{\mathrm{ref}}}\right)^2 \frac{S_{p,s}(r_{\mathrm{eq}})}{S_{p,s}(r_{\mathrm{ref}})}, \tag{9}$$

where $S_{p,s}(r_{\mathrm{ref}})$ and $S_{p,s}(r_{\mathrm{eq}})$ represent the solid phantom scatter factors evaluated for the standard field and phantom dimensions and the scaled field and phantom dimensions, respectively. In Eq. (9) both z_{ref} and z_{eq} are expressed in centimeters.

The reference depth z_{ref} and reference field size r_{ref} in water phantom and the equivalent depth z_{eq} and field size r_{eq}

in solid phantom are scaled in the inverse ratio of relative electron densities (ρ_e) of the two phantom materials (water and solid phantom) as follows:

$$\frac{z_{\mathrm{eq}}}{z_{\mathrm{ref}}} = \frac{\rho_e(w)}{\rho_e(s)} \text{ and } \frac{r_{\mathrm{eq}}}{r_{\mathrm{ref}}} = \frac{\rho_e(w)}{\rho_e(s)}. \tag{10}$$

Typically, the reference depth z_{ref} in water for photon beams is 10 cm, resulting in an equivalent depth z_{eq} of 9.89 cm for Solid Water™ and 8.70 cm for Lucite.

At the depth of calibration, where conditions of transient electronic equilibrium exist, photon energy fluence at a point in a medium is related to the absorbed dose in the medium by the following relationship:

$$D_{\mathrm{med}} = \Psi_{\mathrm{med}} \left(\frac{\bar{\mu}_{\mathrm{en}}}{\rho} \right)_{\mathrm{med}} \beta_{\mathrm{med}}, \tag{11}$$

where Ψ_{med} represents the photon energy fluence at the given point in the medium; $(\overline{\mu_{\mathrm{en}}}/\rho)_{\mathrm{med}}$ the average mass-energy absorption coefficient of the medium; and β_{med} the ratio of absorbed dose and collision kerma at the given point in the medium.

Using Eq. (10) for water (w) and solid phantom (s), the ratio between the dose-to-solid phantom at z_{eq} and the dose to water at z_{ref} for equivalent irradiation geometries can be determined as follows:

$$\frac{D_w(z_{\mathrm{ref}}, r_{\mathrm{ref}})}{D_s(z_{\mathrm{eq}}, r_{\mathrm{eq}})} = \frac{\psi_w}{\psi_s} \frac{(\overline{\mu_{\mathrm{en}}}/\rho)_w}{(\overline{\mu_{\mathrm{en}}}/\rho)_s} \frac{\beta_w}{\beta_s} \equiv \Psi_s^w \left(\frac{\bar{\mu}_{\mathrm{en}}}{\rho} \right)_s^w \beta_s^w. \tag{12}$$

Since the Compton effect is the predominant mode of megavoltage photon interaction with low atomic number absorbers, according to the scaling theorem, the fluence in water at z_{ref} and the fluence at the equivalent point in solid phantom z_{eq} for the same field size r_{ref} are related through Eq. (9). This means that the dose ratio in Eq. (12) can be calculated by taking the ratio of the mass-energy absorption coefficients and β in the two materials in conjunction with an inverse square correction to account for the difference in source-chamber center distance. The dose conversion ratio (or factor) D_w/D_s is then given as follows:

$$\frac{D_w(z_{\mathrm{ref}}, r_{\mathrm{ref}})}{D_s(z_{\mathrm{eq}}, r_{\mathrm{ref}})} = \left(\frac{f + z_{\mathrm{eq}}}{f + z_{\mathrm{ref}}} \right)^2 \left(\frac{S_{p,s}(r_{\mathrm{eq}})}{S_{p,s}(r_{\mathrm{ref}})} \right) \left(\frac{\overline{\mu_{\mathrm{en}}}}{\rho} \right)_s^w \beta_s^w. \tag{13}$$

Applying Eq. (13) to Eq. (6) results in the following expression for the solid phantom-to-water dose conversion factor $k_{s,w}^Q$:

$$k_{s,w}^Q = \left(\frac{f + z_{\mathrm{eq}}}{f + z_{\mathrm{ref}}} \right)^2 \left(\frac{S_{p,s}(r_{\mathrm{eq}})}{S_{p,s}(r_{\mathrm{ref}})} \right) \left(\frac{\bar{\mu}_{\mathrm{en}}}{\rho} \right)_s^w \beta_s^w \left(\frac{\left(\frac{\bar{L}}{\rho} \right)_{\mathrm{air}}^s P_{Q,s}}{\left(\frac{\bar{L}}{\rho} \right)_{\mathrm{air}}^w P_{Q,w}} \right). \tag{14}$$

We analyzed the dose conversion ratio using Eq. (13) and compared this approach to a direct Monte Carlo calculation of the dose ratio water to solid at depths scaled through the relative electron densities of the solid phantom material and water as given by Eq. (9). In addition, Monte Carlo-calculated mass energy absorption coefficient ratios and stopping power ratios were determined for the purpose of evaluating the ratios of stopping power ratios and the ratios of chamber correction factors and, ultimately, the solid phantom conversion factor expressed in Eq. (14).

D. Measurement of $k_{s,w}^Q$ for megavoltage photon beams

Experimentally, from Eq. (7) and using the depth scaling outlined above, the solid phantom conversion factor can be measured as a ratio of ionization chamber readings M_w^Q and M_s^Q corrected for influence quantities in the water phantom at depth z_{ref} and the solid phantom at depth z_{eq}, respectively,

$$k_{s,w}^Q = \frac{M_w^Q}{M_s^Q}. \tag{15}$$

An experimental determination of this conversion factor for a specific phantom is therefore simple and straightforward.

III. MATERIALS AND METHODS

A. Phantoms and ionization chambers

The measurements in water were in a phantom tank of $30 \times 30 \times 30$ cm^3. Solid phantoms with dimensions $20 \times 20 \times 20$ cm^3 were machined from Solid Water™ material (SW, RMI-457) for which several lots were available under the label "certified grade." For these lots, the individual mass density, composition, and electron density are specified by the manufacturer. In addition, evidence is provided that the material is of uniform composition. We also machined a Lucite poly methyl metacrylate (PMMA) phantom of the same dimensions (density $\rho = 1.19$ g/cm^3) from PMMA slabs. It should be noted that the solid phantom dimensions do not represent the electron density scaled dimensions of the water phantom as is required for applying the scaling theorem. However, the slight lack in phantom scattering as a result of this is estimated to be less than 0.1% at the measurement depth for the field sizes used and was ignored.

Holes for insertion of cylindrical ionization chambers were drilled into all phantoms at appropriate depths. Sleeves of the same plastic were machined in order to provide a tight fit of the chamber thimble into the plastic phantom. For the photon phantoms, the point of measurement of the chamber was set at 10 g/cm^2, scaled by the electron density of the individual phantom. All phantoms were irradiated with photon beams at a SSD of 100 cm.

The cylindrical ionization chambers used in this study were of the type Exradin A12 (C552 wall and central electrode) with SN 307, 308, 309, and 310. The chambers were connected to an electrometer (Keithley, model 6517A, Solon, Ohio).

B. Cross calibration of chambers at cobalt-60 gamma rays

The first step toward any clinical implementation of an absorbed dose protocol is to obtain an absorbed dose-in-

TABLE I. Ratios of restricted collision stopping powers material *m* to *air* at the scaled reference depth in the material *m* as a function of megavoltage photon beam quality for the materials water, Solid Water™ (RMI 457), carbon (C), C552, and Lucite (PMMA).

$\%\mathrm{dd}(10)_x$	$(\bar{L}/\rho)^m_{\mathrm{air}}$				
	Water	Solid Water™ (RMI 457)	C	C552	PMMA
^{60}Co	1.1336	1.1113	1.0039	0.9961	1.1025
66.7	1.1201	1.0969	0.9883	0.9840	1.0880
73.0	1.1078	1.0830	0.9767	0.9730	1.0753
77.4	1.0975	1.0723	0.9648	0.9640	1.0631
81.0	1.0890	1.0640	0.9592	0.9563	1.0560
83.5	1.0824	1.0548	0.9505	0.9490	1.0475

water cobalt-60 calibration coefficient for the secondary standard ionization chamber in the clinic from a standards laboratory [e.g., Accredited Dosimetry Calibration Laboratories (ADCLs), National Institute of Standards and Technology (NIST) in the U.S., or National Research Council (NRC) in Canada]. The secondary standard chamber is used to obtain calibration coefficients for all other chambers used routinely in the clinic by comparing, in a cobalt-60 beam, the response of the secondary standard chamber with that of the chamber to be calibrated. In our case the secondary standard is a NE2561 chamber which carries more than 30 years of calibration data on exposure/air-kerma calibration coefficients and only recently absorbed dose calibration coefficients. Hence, frequent use of this chamber in water is avoided by transferring its absorbed dose calibration coefficient, obtained at the NRC, to a set of waterproof, tertiary standard chambers available in our clinic. This procedure was performed in a specifically designed cross-calibration phantom suitable for irradiation in a horizontal beam. We tested the cross-calibration procedure by applying it to an Exradin A12 chamber that had also been calibrated directly at the primary standards dosimetry laboratory and found the agreement to be well within 0.1%.

TABLE II. Ratios of mass-energy absorption coefficients phantom material to chamber wall material as a function of megavoltage photon beam quality for phantom materials water (W), Solid Water™ (RMI 457), and PMMA and for wall materials C552, Carbon (C), and Lucite (PMMA).

$\%\mathrm{dd}(10)_x$	$(\bar{\mu}_{en}/\rho)^w_{\mathrm{wall}}$	$(\bar{\mu}_{en}/\rho)^{\mathrm{SW}}_{\mathrm{wall}}$	$(\bar{\mu}_{en}/\rho)^{\mathrm{PMMA}}_{\mathrm{wall}}$
		Wall=C552	
^{60}Co	1.112	1.079	1.087
66.7	1.109	1.074	1.076
73.0	1.106	1.070	1.066
77.4	1.104	1.062	1.059
81.0	1.099	1.054	1.053
83.5	1.096	1.048	1.048
		Wall=C	
^{60}Co	1.113	1.081	1.082
66.7	1.112	1.077	1.079
73.0	1.119	1.082	1.078
77.4	1.122	1.080	1.077
81.0	1.125	1.079	1.077
83.5	1.126	1.077	1.077
		Wall=PMMA	
^{60}Co	1.029	0.999	1.000
66.7	1.031	0.998	1.000
73.0	1.037	1.003	1.000
77.4	1.043	1.003	1.000
81.0	1.045	1.001	1.000
83.5	1.046	1.000	1.000

C. Measurement of $k^Q_{s,w}$

The solid phantom conversion factor $k^Q_{s,w}$ was measured for cobalt-60 photons, and megavoltage x-ray beams produced by various linear accelerators [Clinac 18 (10 MV), Clinac 2300 (6 and 18 MV), Clinac 6EX (6 MV), and Clinac 21EX (6 and 18 MV); Varian, Palo Alto, California]. The tertiary standard Exradin A12 (SN 307, 308, 309, 310) chambers were used for this purpose and both solid phantoms and water phantom were irradiated in the vertical beam setup. Measurements were corrected for ion recombination, polarity, and environmental conditions in seven solid (six Solid Water™ and one Lucite) phantoms and one water phantom using the procedures recommended in the AAPM TG-51 protocol. As the linac output per monitor unit varies by a few tenths of a percent during one day of irradiations, in-water and in-solid phantom setups were made side-by-side and output per (linac) monitor was checked for constancy. In addition, care was taken that the temperature of the plastic phantoms was accurately monitored as it occasionally, depending on how the phantom was stored, could differ from the water temperature by a few degrees. Finally $k_{s,w}$ was determined by application of Eq. (15) using fully corrected chamber readings.

D. Monte Carlo calculation of $k_{s,w}$

To calculate $k_{s,w}$ using Eq. (6) we evaluated ratios of absorbed doses at scaled depths in the water and solid phantoms. We also calculated ratios of restricted collision stopping powers for the application of cavity theory in both water and the solid phantoms. Ratios of average restricted collision stopping power combined with ratios of average mass energy absorption coefficients are involved in the evaluation of wall correction factors in water and solid phantoms. Finally we also assessed the ratio of gradient corrections in water and solid phantoms as to their contribution to the replacement correction factors.

We used different user codes (see below) from the EGSnrc (Ref. 15) Monte Carlo system to assess the different mentioned components of the phantom dose conversion factor. Some of the accelerator beams used in this work (the in-house accelerator beams) were simulated using the BEAMnrc (Ref. 16) code system. Furthermore, as detailed below, various different user codes have been used to calculate other quantities such as stopping power ratios, mass energy absorption coefficient ratios, and absorbed dose in water, Solid Water™, and Lucite. All phantom calculations use transport kinetic energy cutoff values of 10 keV for electrons and photons, whereas respective cutoff values of 189 and 100 keV were used to generate the BEAMnrc phase space files and spectra.

1. Ratios of average restricted collision stopping power

Ratios of averaged restricted collision stopping powers are involved in both the dose conversion from cavity to medium as well as in the chamber wall correction factors needed to evaluate the phantom dose conversion factor. Stopping power ratios water to air, solid to air, water to wall, and solid to wall were evaluated using the SPRRZnrc user code[17] of the EGSnrc code system[15] for water, Solid Water™, and Lucite as phantom materials. We used both in-house spectra for the accelerator beams generated using the BEAMnrc system as well as spectra kindly provided by Sheikh-Bagheri and Rogers[18] for intermediate points. All calculations were performed at scaled depths in each of the phantoms and expressed as a function of the beam quality $\%dd(10)_x$. Table I summarizes the stopping power ratios phantom material to air, for water, Solid Water™, C552, carbon, and Lucite (PMMA).

2. Ratios of average mass energy absorption coefficients

Table II summarizes ratios of mass-energy absorption coefficients, phantom material to chamber wall material, as a function of megavoltage photon beam quality for phantom materials water (W), Solid Water™ (RMI 457), and PMMA and for wall materials C552, carbon (C), and Lucite (PMMA). These were calculated by averaging mass energy absorption coefficients over the photon fluence spectra at a depth of 10 cm in water and at scaled depths in Solid Water™ and Lucite. These mass energy absorption coefficient ratios are involved in the calculation of wall correction factors in water and in Solid Water™ and Lucite. For consistency these were calculated using photon fluence spectra resulting from full accelerator simulations using the BEAMnrc code for the available in-house accelerator beams as well as from spectra kindly provided by Sheikh-Bagheri and Rogers.[18] Mass energy absorption coefficients averaged over the photon energy fluence were calculated in-the flight using the EGSnrc/G user code which scores the energy transferred by photons in the material of interest and corrects for radiative loss by tracking charged particle slowing down in the material and scoring the energy fraction expended in radiative processes.

3. Wall correction factors

Wall correction factors in water, Solid Water™, and Lucite were calculated with the two component model[19] using the stopping power ratios and mass energy absorption coefficient ratios determined as described above. To this end use was made of the data by Lempert *et al.*[20] of the fraction of ionization contributed to the cavity dose by interactions occurring in a wall of a given thickness of material. We used the Lempert *et al.*[20] data as plotted in the IAEA-277 code of practice as a function of (TPR) where we used the shifted TPR axis so that it starts at 0.60 rather than 0.65.[21] TPR was converted $\%dd(10)_x$ using the relation published by Kalach and Rogers,[22] valid for clinical beams. Wall correction factors and their ratios for Solid Water™ and Lucite to water for an Exradin A12 chamber are summarized in Table III(a). Note the significantly increased magnitude of the wall correction when the phantom material is Solid Water™. In the phantom dose conversion factor, these ratios represent a correction of up to 0.6% for Solid Water™ and up to 0.3% for Lucite.

4. Replacement correction factors

The replacement correction factor consists of two components, a gradient correction factor and a fluence perturbation correction factor, the latter of which is assumed unity in high energy photon beams. We evaluated ratios of gradient correction factors for a Farmer-type ionization chamber in Solid Water™ and Lucite as phantom materials relative to water as a function of beam quality. Replacement correction factors and their ratios in solid phantoms and water are shown in Table III(b) and it can be seen that their ratio is limited to 0.1% or less.

IV. RESULTS AND DISCUSSION

A. Dose conversion ratio from Solid Water™ and Lucite to water

For accurate calculations of the phantom scaling correction factors we evaluated the dose conversion ratio $D_w(z_{\mathrm{ref}}, r_{\mathrm{ref}})/D_s(z_{\mathrm{eq}}, r_{\mathrm{ref}})$ using direct Monte Carlo calculations of ratio of dose to water to dose to solid phantoms Solid Water™ and Lucite (PMMA). In addition, to assess the accuracy of Eq. (13) that expresses this dose conversion ratio as a product of ratios of interaction coefficients, scatter factors and an inverse square correction, we compared the application of Eq. (13) with the direct Monte Carlo calculation of the dose ratio and the results are shown in Fig. 1. Note that in the application of Eq. (13) the ratio, β_s^w has been ignored. This comparison shows that Eq. (13) leads to calculations of dose ratios water to solid that are accurate to within 0.4% for Solid Water™ and Lucite which means that, within this uncertainty, this factor can be calculated using basic interaction data.

TABLE III. Wall correction factors and replacement correction for an Exradin A12 ionization chamber in water, Solid Water™ (RMI 457), and Lucite phantoms as a function of megavoltage photon beam quality. The two rightmost columns show ratios of wall correction factors and replacement correction factors in the solid phantoms relative to water as used in the calculations of $k^Q_{s,w}$. The Exradin A12 chamber has a C552 wall of 0.088 g cm^{-2} thickness and an internal diameter of 6.1 mm.

		(a) Wall correction factor			
$\%dd(10)_x$	Water	Solid water	Lucite (PMMA)	$(P_{wall})^{SW}_w$	$(P_{wall})^{PMMA}_w$
^{60}Co	0.985	0.979	0.985	0.994	1.000
66.7	0.989	0.984	0.988	0.995	0.999
73.0	0.992	0.989	0.990	0.997	0.998
77.4	0.993	0.989	0.991	0.997	0.998
81.0	0.993	0.989	0.990	0.996	0.997
83.5	0.992	0.988	0.990	0.996	0.998
		(b) Replacement correction factor			
^{60}Co	0.9894	0.9873	0.9862	1.0002	0.9991
66.7	0.9909	0.9895	0.9889	1.0001	0.9995
73.0	0.9916	0.9909	0.9903	1.0000	0.9993
77.4	0.9922	0.9917	0.9911	1.0001	0.9995
81.0	0.9872	0.9920	0.9918	0.9998	0.9996

B. Phantom dose conversion correction factor for Solid Water™ and Lucite

Figure 2 shows the phantom dose conversion factors for Solid Water™ and Lucite as a function of beam quality. Measurements using different solid phantoms of the same type (Solid Water™, RMI-457, certified grade) are shown in dashed lines, calculations are shown in full lines. The main graph is for Solid Water™ whereas the inset is for Lucite as phantom material. For Solid Water™, the maximum difference between measurement and calculation is 0.7% at ^{60}Co and 0.6% at 18 MV photons. The average difference between measurement and calculation is 0.3%, the calculation being, on average, higher than the measurements. This result suggests that measurements of dose at scaled depths in Solid Water™ are consistent with dose measurements in water to within 0.7%. McEwen and Niven[23] show an even more optimistic result for the material virtual water where, upon suitable range scaling, photon, and electron dosimetry in a solid phantom gave agreement with that in water within 0.2%.

However, Fig. 3 shows a charge transfer (CT) slice through the center of one of our Solid Water™ phantoms. Clearly visible are the chamber details, the insert for the thermometer, the Solid Water™ sleeve, and the gaps between chamber and sleeve, sleeve and phantom, and between different phantom blocks. Also visible are nonhomogeneous areas and air pockets in the phantom resulting from the construction process of the phantom. For phantoms consisting of blocks joined together, there is also a distinct possibility that, depending on the phantom construction, there are gaps in the path of the primary beam. This may lead to an actual depth of the measuring point in Solid Water™ being smaller than

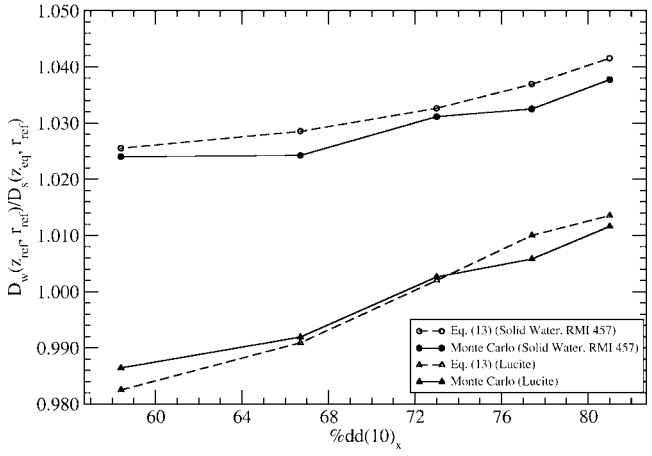

FIG. 1. Dose conversion factor $D_w(z_{ref}, r_{ref})/D_s(z_{eq}, r_{ref})$ evaluated using Eq. (13) (dashed lines) or using direct Monte Carlo calculations (full lines) for Solid Water™ (RMI 457; circles) and for Lucite (triangles). In the application of Eq. (13) the ratio β^w_s has been ignored.

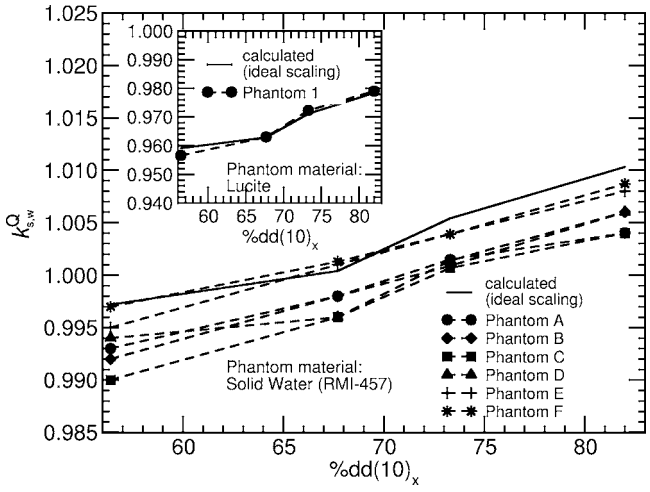

FIG. 2. Phantom dose conversion factor for photon beams $k^Q_{s,w}$ for six Solid Water™ (Gammex RMI 457) and the Lucite (PMMA) phantoms (inset) as a function of beam quality expressed in $\%dd(10)_x$. Dashed lines: measurements; full line: calculations.

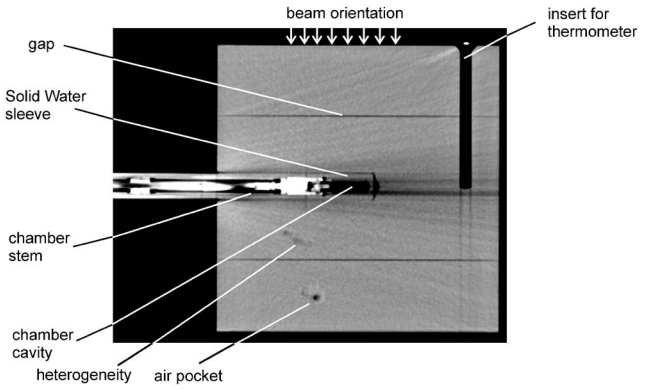

FIG. 3. CT image of a Solid Water™ phantom with Farmer-type chamber in Solid Water™ sleeve. Shown are inset for thermometer, nonhomogeneous areas as well as the gap in the path of the beam occurring as a result of joining different blocks of Solid Water™.

the nominal measurement depth and would give rise to measured phantom scaling factor $k_{s,w}$ that is slightly lower than the calculated factor. The magnitude of the discrepancy depends on how large the overall gap is; an air gap of 1 mm as suggested by the CT scan would lead to a difference of around 0.3% to 0.5%. We could not rule out that all Solid Water™ phantoms used in this work had gaps in the path of the beam that were consistent with the discrepancy between measured and calculated $k_{s,w}$ factors. Hence, 0.3% to 0.5% discrepancies with doses obtained through in-water measurements and the TG-51 protocol should be considered to be within uncertainties. We therefore recommended that plastic phantoms are constructed such that gaps in the path of the beam are avoided.

For the Lucite phantom we found that the agreement between measured and calculated phantom dose conversion factors was better and within 0.2% for all radiation qualities despite the fact that the scaling involves differences in depth that are much larger than in the case of Solid Water™. It is possible that for Lucite the stated material density and composition agrees better with the true composition and that, since the construction process is different, the material homogeneity is better than Solid Water™. More work with different Lucite phantoms is required to confirm the reproducibility of these results. Solid Water™ on the other has the advantage that the magnitude of the phantom dose conversion factor is very close to unity. A phantom dose conversion factor of unity can be interpreted as a numerical expression of perfect water equivalence. Our results show that for the majority of the Solid Water™ phantoms used, water equivalence is achieved to within 0.5%, which is consistent with the manufacturer stated tolerance of "certified grade" Solid Water™. However, we suggest that every solid phantom be experimentally investigated for water equivalence before it is used for the verification of reference dosimetry.

The use of Eq. (13) instead of Monte Carlo calculated dose ratios (as used in Fig. 2) would worsen the agreement by, on average, 0.4%. This still means that the agreement between measured and calculated dose by using Eq. (14) would, on average, be within 0.7% for Solid Water™ and within 0.5% for Lucite.

Finally we would like to point out that with the procedures outlined in this paper, we are not advocating the use of plastic phantoms for clinical reference dosimetry; these should be performed according to the recommendations of TG-51 or IAEA TRS-398, i.e., in liquid water. Instead we provide conditions under which absorbed dose to water can be measured using solid phantoms combined with a formalism similar to TG-51 or IAEA TRS-398 corrected using an experimentally determined phantom dose conversion factor. By experimentally determining the phantom dose conversion factor, the potential variability in plastic phantom materials of the same type is incorporated in the procedure while the results of the in-solid phantom measurement can be interpreted in a physically meaningful way. Alternatively, by comparing measured and calculated phantom conversion factors the suitability of a given plastic for the purpose of clinical reference dosimetry can be investigated.

V. CONCLUSIONS

In this paper we present a framework within which ionization chambers, calibrated in terms of absorbed dose to water, can be used to determine absorbed dose to water under reference conditions from a measurement in a solid phantom of known density and composition. Such a procedure has the distinct advantage that measurements in plastics can be done under conditions that simplify the interpretation of the chamber signal and make the conversion to absorbed dose to water under reference conditions direct and straightforward. We define a phantom dose conversion factor that relates an absorbed dose-to-water calibration coefficient to an in-solid phantom absorbed dose-to-water calibration coefficient valid at a depth scaled by electron density. For an Exradin A12 C552 ionization chamber, we calculated and measured the phantom dose conversion factor for a set of Solid Water™ phantoms and found that measured and calculated factors differed by between 0.0% and 0.7% and the average measured dose conversion factor was low by 0.4% compared to the calculated factor. For the one Lucite phantom tested the difference was 0.2% or less for all energies. The magnitude of a difference between measurement and calculation depends on the consistency of phantom composition with the composition assumed in the calculations and on the phantom homogeneity and construction in the experiments. When these are independently verified by the user in accurate experiments for each phantom used, dose measurements using ionization chambers calibrated in terms of absorbed dose to water lead to reference dose determinations that are consistent with in-water measurements and absorbed dose-based protocols to within a few tenths of a percent. As the calculation of phantom dose conversion factors for different chamber types in combination with different phantom materials is straightforward, a more general availability of these factors for different chamber types and phantom materials could be useful.

ACKNOWLEDGMENTS

We thank Dr. Daryoush Sheikh-Bagheri and Dr. D. W. O. Rogers for kindly providing their x-ray spectra in digital format. We acknowledge funding from grants from the Natural Sciences and Engineering Research Council (NSERC, RG-PIN 298191) and from the Canadian Institutes of Health Research (CIHR, MOP 57 828). J.S. is a research scientist of the National Cancer Institute of Canada (NCIC) appointed with funds provided by the Canadian Cancer Society (CCS).

[a]Electronic mail: jseuntjens@medphys.mcgill.ca

[1]P. R. Almond, P. J. Biggs, B. M. Coursey, W. F. Hanson, M. Saiful Huq, R. Nath, and D. W. O. Rogers, AAPM's "TG-51 protocol for clinical reference dosimetry of high-energy photon and electron beams," Med. Phys. **26**, 1847–1870 (1999).

[2]P. Andreo, D. T. Burns, K. Hohlfeld, M. S. Huq, T. Kanai, F. Laitano, V. G. Smyth, and S. Vynckier, "Absorbed dose determination in external beam radiotherapy: An international code of practice for dosimetry based on absorbed dose to water," Technical Report Series No. 398, International Atomic Energy Agency, 2000.

[3]O. S. Dohm, G. Christ, F. Nüsslin, E. Schüle, and G. Bruggmoser, "Electron dosimetry based on the absorbed dose to water concept: A comparison of the AAPM TG-51 and DIN 6800-2 protocols," Med. Phys. **28**, 2258–2264 (2001).

[4]M. S. Huq, H. Song, P. Andreo, and C. J. Houser, "Reference dosimetry in clinical high-energy electron beams: Comparison of the AAPM TG-51 and AAPM TG-21 dosimetry protocols," Med. Phys. **28**, 2077–2087 (2001).

[5]M. S. Huq and P. Andreo, "Reference dosimetry in clinical high-energy photon beams: Comparison of the AAPM TG-51 and AAPM TG-21 dosimetry protocols," Med. Phys. **28**, 46–54 (2001).

[6]G. X. Ding, J. E. Cygler, and C. B. Kwok, "Clinical reference dosimetry: Comparison between AAPM TG-21 and TG-51 protocols," Med. Phys. **27**, 1217–1225 (2000).

[7]AAPM TG-21, "A protocol for the determination of absorbed dose from high-energy photon and electron beams," Med. Phys. **10**, 741–771 (1983).

[8]IAEA International Atomic Energy Agency, "Absorbed dose determination in photon and electron beams: An International Code of Practice," Technical Report Series No. 277, 2nd ed. (IAEA, Vienna, 1987).

[9]D. T. Burns, M. R. McEwen, and A. J. Williams, "An NPL absorbed dose calibration service for electron beam radiotherapy," *Proc. Int. Symp. on Measurement Assurance in Dosimetry* (IAEA-SM-330/34) edited by S. P. Flitton (Vienna, IAEA, 1994), p. 61.

[10]IPEMB "The IPEMB code of practice for electron dosimetry for radiotherapy beams on initial energy from 2 to 50 MeV based on an air kerma calibration," Phys. Med. Biol. **41**, 2557–2603 (1996).

[11]IPEM, "The IPEM code of practice for electron dosimetry for radiotherapy beams of initial energy from 4 to 25 MeV based on an absorbed dose to water calibration," Phys. Med. Biol. **48**, 2929–2970 (2003).

[12]J. S. Pruitt and R. Loevinger, "The photon-fluence scaling theorem for Compton-scattered radiation," Med. Phys. **9**, 176–179 (1982).

[13]R. F. Nutbrown, S. Duane, D. R. Shipley, and R. A. S. Thomas, "Evaluation of factors to convert absorbed dose calibrations from graphite to water for the NPL high-energy photon calibration service," Phys. Med. Biol. **47**, 441–454 (2002).

[14]R. F. Nutbrown, M. R. McEwen, R. A. S. Thomas, S. Duane, and D. R. Shipley, "Comparison of conversion factors for X-ray beams from a Philips SL15 and the NPL linear accelerator," Phys. Med. Biol. **46**, N245–N252 (2001).

[15]I. Kawrakow and D. W. O. Rogers, "The EGSnrc code system: Monte Carlo simulation of electron and photon transport," Technical Report PIRS-701, National Research Council of Canada, Ottawa, Canada, 2000; see http://www.irs.inms.nrc.ca/inms/irs/EGSnrc/EGSnrc.html.

[16]D. W. O. Rogers, B. A. Faddegon, G. X. Ding, C.-M. Ma, J. We, and T. R. Mackie, "BEAM: A Monte Carlo code to simulate radiotherapy treatment units," Med. Phys. **22**, 503–524 (1995).

[17]D. W. O. Rogers, I. Kawrakow, J. P. Seuntjens, and B. R. B. Walters, "NRC user codes for EGSnrc," Technical Report PIRS-702, National Research Council of Canada, Ottawa, Canada, 2000.

[18]D. Sheikh-Bagheri and D. W. O. Rogers, "Monte Carlo calculation of nine megavoltage photon beam spectra using the BEAM code," Med. Phys. **29**, 391–402 (2002).

[19]P. R. Almond and H. Svensson, "Ionization chamber dosimetry for photon and electron beams," Acta Radiol.: Ther., Phys., Biol. **16**, 177–186 (1977).

[20]G. D. Lempert, R. Nath, and R. J. Schulz, "Fraction of ionization from electrons arising in the wall of an ionization chamber," Med. Phys. **10**, 1–3 (1983).

[21]M. S. Huq and R. Nath, "Comparison of IAEA 1987 and AAPM 1983 protocols for dosimetry calibration of radiotherapy beams," Med. Phys. **18**, 26–35 (1991).

[22]N. I. Kalach and D. W. O. Rogers, "Which accelerator photon beams are "clinic-like" for reference dosimetry purposes?," Med. Phys. **30**, 1546–1555 (2003).

[23]M. McEwen and D. Niven, "Detailed characterization of the water-equivalent material virtual water in high-energy photon and electron beams," *Proceedings World Congress on Medical Physics and Biomedical Engineering*, WC 2003, Sydney (AFOMP, Sydney, 2003).